

Channel  
Current  
Model  
Tide  
Lagrange

Manche  
Courant  
Modèle  
Marée  
Lagrange

# An atlas of long-term currents in the Channel

Jean-Claude SALOMON and Marguerite BRETON

Institut Français de Recherche pour l'Exploitation de la Mer, Centre de Brest,  
Laboratoire Hydrodynamique et Sédimentologie, B.P. 70, 29280 Plouzané,  
France.

## ABSTRACT

A two-dimensional mathematical model was used to compute long-term currents in the Channel. Eleven maps are presented here, corresponding to various tidal coefficients and wind directions.

The last diagram shows the magnitude of the dispersion coefficient. This enables a dilution computation to be added to the advective part of dissolved substances and microorganism movements.

*Oceanologica Acta*, 1993. 16, 5-6, 439-448.

## RÉSUMÉ

### Atlas des courants résiduels en Manche

Un modèle mathématique bidimensionnel est utilisé pour calculer les courants à long terme dans la Manche. Onze cartes sont proposées qui correspondent à des coefficients de marée et des directions de vent différents.

Une dernière planche présente la dispersion. Elle permet de compléter la partie advective du transport de matières dissoutes ou de micro-organismes, par un calcul de dilution.

*Oceanologica Acta*, 1993. 16, 5-6, 439-448.

## INTRODUCTION

The Channel is reputed for its strong tides and the violent currents associated with them. These tidal currents are the main signal on time scales of a few hours and data pertaining to this mesoscale are widely available in various easily accessible documents (*see for example Service Hydrographique et Océanographique de la Marine, 1973*).

However, tidal currents are not the only currents in the Channel, which also has a long-term component on the synoptic scale (of the order of one week to one year) with a much lower intensity. Hence, it is difficult to measure the latter directly, and they are especially perceptible through the slow movement of water masses and the living or inert substances they displace over hundreds of kilometres.

Thus, these currents are relevant to management planning or to the solution of scientific problems involving transport of nutritive chemical or polluting substances, or of microorganisms such as eggs or larvae, for example, over long distances.

In the Channel, these long-term currents are all the more difficult to apprehend in that they are very weak with regard to tidal currents (often one to two orders of magnitude lower) and are largely dependent on weather conditions. Therefore, they are variable and difficult to separate from the background noise in the measurement. However, this is not a general comment, as we will later see that near large topographical irregularities, a constant component of these currents, due to nonlinear effects of the tide create currents so intense that they are hardly disturbed by weather conditions (Pingree and Maddock, 1977 and 1985; Orbi and

Salomon, 1988; Salomon and Breton, 1991). In this case, they have been measured directly and are already known (Pingree and Mardell, 1987).

Elsewhere, this being the most general case in the Channel, all that was available until recently were partial, or even contradictory, experimental indications, often obtained using chemical or biological markers in water masses. Considerable progress has since been made recently on this point, using artificial radioactive markers discharged by the nuclear fuel reprocessing plant at la Hague (Guéguéniat *et al.*, 1988 and 1993). Some of these radionuclides are almost conservative, and because the source is both unique and known, some specific trajectories toward the Norman-Breton gulf or toward the Dover Strait have been detected and rated according to time (Salomon *et al.*, 1991; Guéguéniat *et al.*, 1993 and communication to the Channel Symposium).

But these tracers are not transported over the entire Channel and the measurement effort this method requires has limited the number of measurements taken to about two thousand. Taking into account the natural system's variability and the contribution made by diffusion mechanisms to this transport phenomenon, these measurements have not sufficed for true mapping of water movements.

The determinant contribution comes from the mathematical model which can be used both for theoretical calculations, which help in understanding basic processes, as well as for realistic simulations providing accurate and synthetic descriptions of complicated facts.

Considering the general hydrodynamic conditions in the Channel and the importance given here to time scales higher than that of characteristic vertical mixing time, two-dimensional approximation is acceptable. Thus, the numerical tool has existed for some time, and successive studies have greatly contributed to knowledge. However, in the view of the present authors, they have not succeeded in completely solving the problem, having, at least partially, been confronted with the following two required conditions:

- 1) Having a model which not only provides large enough geographical coverage to escape problems linked to the accuracy of boundary conditions, but which also provides spatial discretization of the order of 2 km or less, so as correctly to describe the movement of water particles during the tidal cycle. This matter could in great measure be resolved by moving the model boundaries away from the area where mechanisms to be studied are generated (in the present case, beyond the shelf break) and by obtaining access to more powerful computers.

- 2) Solving the fundamental difficulty arising from Lagrangian residual currents which, contrary to currents related to a fixed point (Eulerian), do not appear to be single currents in a given location, although outside conditions remain unchanged. Following Longuet-Higgins's (1969) introduction of the idea of mass transport velocity, showing that this was the sum of the Eulerian residual current and Stokes's drift, various important studies have confirmed that water mass displacement cannot be understood from the Eulerian concept. The Lagrangian concept of long-term particle trajectories and

residual current had to be introduced. This was done by Zimmerman (1979) and many authors, including Cheng *et al.* (1986) and Feng (1987 and 1990) then tried to determine its mathematical relation with Eulerian residual currents. They demonstrated the existence of a third current component, Lagrange's drift, which depends on the moment of particle departure.

These fundamental mathematical developments are based on a hypothesis of slight non-linearity of physical systems. In the opposite case, numerical solutions to this problem were sought: Pingree and Maddock (1985), Orbi and Salomon (1988), Salomon *et al.* (1988; 1991 and 1993 *b*), Foreman *et al.* (1992).

When currents and their spatial gradients are particularly intense, which is the case in the Channel, the non-unicity of Lagrange's residual currents, even for an entirely periodic tide, creates problems for use. The authors addressed this difficulty by introducing a new spatial reference: the "barycentric" system, enabling a single current field to be obtained without averaging Lagrange's drift (Salomon *et al.*, 1993 *b*).

From those significant advances, over the past few years, the possibility of mapping long-term water movements has appeared.

In the Channel, results of these calculations were compared with direct velocity measurements (current-meter and drifting buoys) reported by Pingree and Mardell (1987) or Orbi and Salomon (1988) among others, with remote-sensing indications (Pingree, 1984; Boxall and Robinson, 1987; Jégou and Salomon, 1991) and especially with the above-mentioned radioactive tracers (Salomon *et al.*, 1988; Guéguéniat *et al.*, 1993). Crosschecking with biological indicators (population discontinuity, isolation, diversity) known to local marine fauna specialists and widely reported on within research groups (GDR "Manche") and the EEC-MAST *Fluxmanche* programme, was also done whenever possible.

Today these results appear to be sufficiently grounded in theory and verified by experiments to be transmitted to nonspecialized users. Several presentations made at the "Channel Symposium" and republished in this volume have demonstrated their importance, particularly for questions of biology.

## METHOD

The methodology followed here has already been presented as the barycentric method (Orbi and Salomon, 1988; Salomon *et al.*, 1988 and 1993 *b*). Although a complete overview may be found in the more recent of these papers, it will be briefly described below.

### Instantaneous current model

The first step consists in computing instantaneous tidal currents, by solving the Navier-Stokes equations after their integration on the vertical (Saint-Venant equations).

The choice of a numerical method is of little importance. However, because the model will then be used to calculate trajectories of imaginary particles, meshes must be small enough to enable accurate computations of trajectories and of their residual components which are often one or two orders of magnitude lower than the tidal excursion. After a number of tests it was concluded that six discretization intervals were an acceptable lower limit to obtain a correct evaluation of the residual movement.

Average tidal velocities being generally about  $1 \text{ m}\cdot\text{s}^{-1}$ , the model mesh size was chosen equal to one nautical mile.

This 2D model has already been presented in Salomon and Breton (1991). Its geographical limits are defined along meridians  $3^\circ\text{E}$  and  $6^\circ 28'\text{W}$ , and parallels  $48^\circ 18'\text{N}$  and  $51^\circ 20'\text{N}$ . Boundary conditions are obtained from a wider 2D model, working in spherical coordinates from  $12^\circ\text{W}$  to  $12^\circ 30'\text{E}$ , and from  $47^\circ\text{N}$  to  $63^\circ\text{N}$ . The mesh size of the latter is  $10'$  in longitude and  $6'$  in latitude. Boundary conditions were taken from Schwiderski's atlas (1983).

### Lagrange's residual currents

Although the barycentric method has proved to be more general (Salomon *et al.*, 1993 *b*), it will be used here under the simplifying hypothesis of a periodic tide (period  $T$ ), not sinusoidal, and a constant wind field.

For any specific combination of tide and wind, the tidal model is activated until a stationary situation is reached, then used to calculate trajectories over the following two tidal cycles.

From the results of these simulations, and for various  $\alpha$  water particles, each corresponding to a departure point ( $x_0$ ) and a departure time ( $t_0$ ), numerical calculation of Lagrange's residual velocity is performed, defined as follows:

$$\bar{V}_{rl}(x_0, t_0) = \bar{V}_{rl}(\alpha) = \int_{t_0}^{t_0+T} \bar{V}(\alpha, t) dt$$

This operation is repeated for a large number of points spread over the entire field, for instance within each mesh and for several moments of departure ( $t_0$ ) spaced out over the next-to-last tidal cycle mentioned above.

Both theory (Cheng *et al.*, 1986) and numerical experience (Orbi and Salomon, 1988; Foreman *et al.*, 1992) demonstrate that, for each departure point ( $x_0$ ) a series of different values of  $\bar{V}_{rl}(x_0, t)$  corresponding to the various  $t$  values (Fig. 1) are thus obtained.

As for Foreman *et al.*, averaging these vectors over time could be attempted to obtain a single value:

$$\overline{\bar{V}_{rl}(x_0)} = \frac{1}{T} \int_T \bar{V}_{rl}(x_0, t) dt$$

Clearly, by proceeding in this way, part of the movement spectrum from the calculated current field is removed, which then has to be compensated for by increasing dispersion terms. Thus, the formalism of Reynold's stress on the meso-scale, introduced by Ronday (1976) is approximated.

However, this correction attempt is not satisfactory, since the advective components which were to be eliminated represent a water and matter flux in a direction determined by the tide, whereas a diffusion term represents a flux in the direction of the concentration gradient.

An alternative solution was sought by introducing barycentric coordinates.

### Barycentric coordinates

The basic idea behind this method is that a water particle will make only one long term displacement. Therefore, it has only one residual velocity. The difficulty encountered above was due to the fact that residual displacements were assigned to geographical points, which are not characteristic of a particle, unless they are combined with a notion of time: only the ( $x_0, t_0$ ) pair can characterize a particle. So, another single parameter, equivalent to the ( $x_0, t_0$ ) pair was sought.

Following up on ideas from Miche (1944) concerning surface waves, an ideal parameter to characterize a particle could be its position at rest, *i.e.*, its position in the case of a tidal movement whose amplitude would be infinitely small.

In fact, for obvious practical reasons, this position is extremely difficult to determine numerically and is initially replaced by the position of the particle's centre of gravity during the tidal cycle under consideration.

Thus, together with the calculation of each particle's Lagrangian residual velocity, the average position of the particle is calculated simultaneously:  $G(x_0, t_0)$

$$G(x_0, t_0) = x_0 + \frac{1}{T} \int_{t_0}^{t_0+T} \int_{t_0}^t V(\alpha, t') dt' dt$$

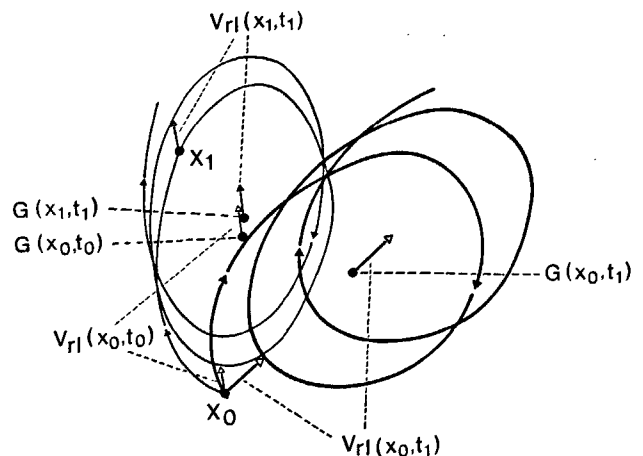


Figure 1

Kinematic elaboration of the Lagrangian residual velocity field in barycentric coordinates.  $x_i$  ( $i = 0; 1$ ) are different points of departure of particles.  $G(x_i, t_i)$  are the centres of gravity of the particle trajectories starting from point  $x_i$  at time  $t_i$ .

Construction cinématique du champ de vitesses résiduelles de Lagrange en coordonnées barycentriques.  $x_i$  ( $i = 0; 1$ ) sont les différents points de départ des particules.  $G(x_i, t_i)$  sont les centres de gravité des trajectoires des particules partant de  $x_i$  au temps  $t_i$ .

The Lagrangian residual velocity is then allocated to this centre of gravity (the barycentre).

This reference modification corresponds to a displacement of each of the beam vectors  $\vec{V}_{rl}(x_0, t)$  which become separated and approximately distributed along the edges of an ellipse centred on point  $x_0$  [points G ( $x_0, t_0$ ) and G ( $x_0, t_1$ ) on Figure 1].

Gathering at the same point or immediately beside it, other  $\vec{V}_{rl}$  vectors are observed which in fact involve the same water mass, but were determined by releasing particles at other moments, and other locations distributed along the same particle trajectory (point  $x_0$  at time  $t_1$ , on Figure 1).

Conversely, particles released at the same departure point  $x_0$ , but at time  $t_1$  (different from  $t_0$ ) will undergo a distinct trajectory and probably a different residual velocity.

This latter vector will be allocated to a different centre of gravity G ( $x_0, t_1$ ) [on Fig. 1].

Lastly, it was numerically verified (Orbi and Salomon, 1988), that vectors gathering in the same area were nearly identical. However, small discordances observed in some places were initially attributed to inaccuracies in the construction of tidal trajectories, but may also be related to the movement's chaotic part set out by Ridderinkhof and Zimmerman (1992). While the question was not solved, probably because our computations are limited to only one tidal cycle, these discrepancies were always found to be very small and could easily be included in the dispersive part of the movement.

The current field thus obtained could be used, as such, to calculate displacements or residence time, with the precaution of effecting a transposition between true space and the new coordinate system. Thus, a particle released at  $x_0$ , at the moment  $t_0$ , would undergo a spatial translation, and a series of particles successively released at the same  $x_0$  spot would be set apart from each other in the new reference. Each one is placed at the centre of gravity of the movement defined during a tidal cycle. An inverse conversion then has to be made to return to true space.

As this velocity field is stationary, it might be non-divergent, but because of its kinematic elaboration which does not explicitly involve the notion of mass conservation, this is not absolutely true everywhere. This especially fails near capes where the particle's average position (which we compute) may be quite different from its position at rest (which we are seeking). An iterative procedure is then used to minimize the divergence of the velocity field.

At the outcome of the latter operation, a single Lagrangian residual velocity field is finally obtained, very close to the previous one, yet non-divergent, thus enabling the advection-dispersion equation to be solved by a conservative numerical method, as those relating to the control volume approach.

Such computations have been done, for a semi-diurnal periodic tide ( $T = 12.42$  h) coming from the ocean. Residual velocity fields are presented in the following as trajectories (in black) drawn over a coloured background indicating the movement intensity (in  $m \cdot s^{-1}$ ).

## RESULTS AND DISCUSSION

### Currents

Ten maps are presented below (Fig. 2-11), concerning:

Map 2: average tide, no wind	$\phi = 37\,400 \text{ m}^3\text{s}^{-1}$
Map 3: spring tide, no wind	$\phi = 75\,500 \text{ m}^3\text{s}^{-1}$
Map 4: average tide, north wind	$\phi = -104\,800 \text{ m}^3\text{s}^{-1}$
Map 5: average tide, northeast wind	$\phi = -73\,700 \text{ m}^3\text{s}^{-1}$
Map 6: average tide, east wind	$\phi = 22\,500 \text{ m}^3\text{s}^{-1}$
Map 7: average tide, southeast wind	$\phi = 127\,400 \text{ m}^3\text{s}^{-1}$
Map 8: average tide, south wind	$\phi = 180\,000 \text{ m}^3\text{s}^{-1}$
Map 9: average tide, southwest wind	$\phi = 148\,500 \text{ m}^3\text{s}^{-1}$
Map 10: average tide, west wind	$\phi = 52\,300 \text{ m}^3\text{s}^{-1}$
Map 11: average tide, northwest wind	$\phi = -52\,600 \text{ m}^3\text{s}^{-1}$

Flow through the Dover Strait was calculated for each of these situations. Results are reported above, as  $\phi$  values.

In the centre of the Channel, currents are nearly parallel and oriented to the east or to the west, depending on the north-south component of the wind. Velocities are very weak in the western part of the Channel and higher in the east, the maximum being in the Dover Strait.

On both sides there are many tidally-induced gyres, especially near the Isle of Wight, Portland Bill, Cap de la Hague, the Seine Bay and the Norman-Breton gulf. The weakest gyres are easily destroyed by the wind, but the stronger ones, around the British Isles, persist in all weather situations considered here.

A reminder that these are water particle trajectories, expressed in barycentric coordinates, *i.e.* located according to their average position during the tide cycle. This, under the simplifying hypothesis of constant, uniform wind, a constant tidal coefficient and a two-dimensional calculation. Wind velocity is about 8 m/s, thus creating a surface stress of 0.13 Pa.

These hypothesis require that the following precautions be taken:

- The tidal current's phase and intensity must be taken into account to link the average position of a mobile particle in the barycentric system to its true position at any given moment.
- The response time of the Channel's hydrodynamic system, coupled with the North Sea, being around four days (*see Salomon et al., 1993 a*), average weather conditions, at least, on this time scale, must be considered.
- Wind pressure being a quadratic function of speed, the quadratic average of winds must be used.

The two-dimensional calculation hypothesis, though generally accepted for the Channel, leads us to take certain precautions in areas where notable temporary stratifications exist.

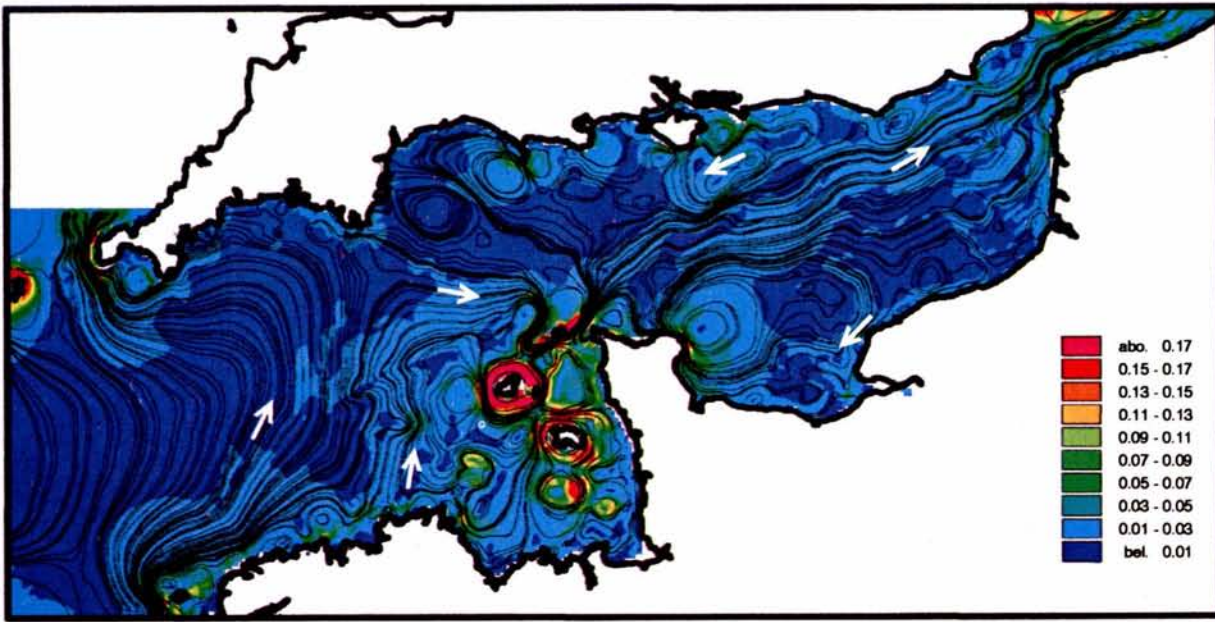


Figure 2  
Long-term trajectories and velocity of water movement for an average tide and no wind.

Trajectoires et intensités des courants à long terme, pour une marée moyenne, sans vent.

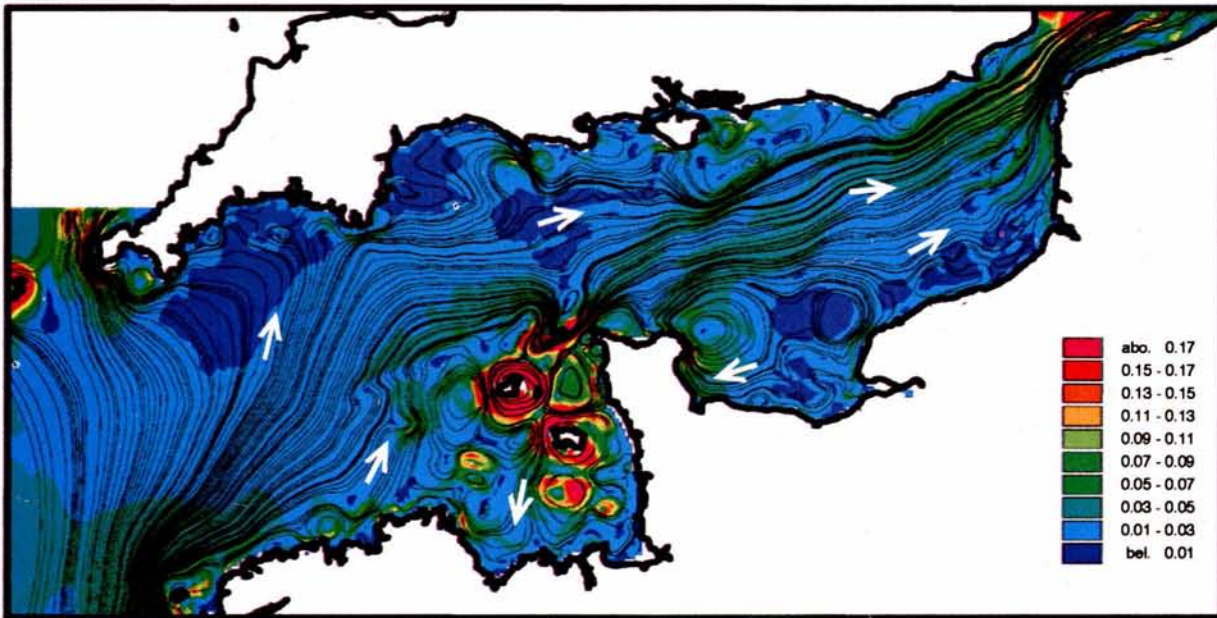


Figure 3  
Long-term trajectories and velocity of water movement for a spring tide and no wind.

Trajectoires et intensités des courants à long terme, pour une marée de vive eau, sans vent.

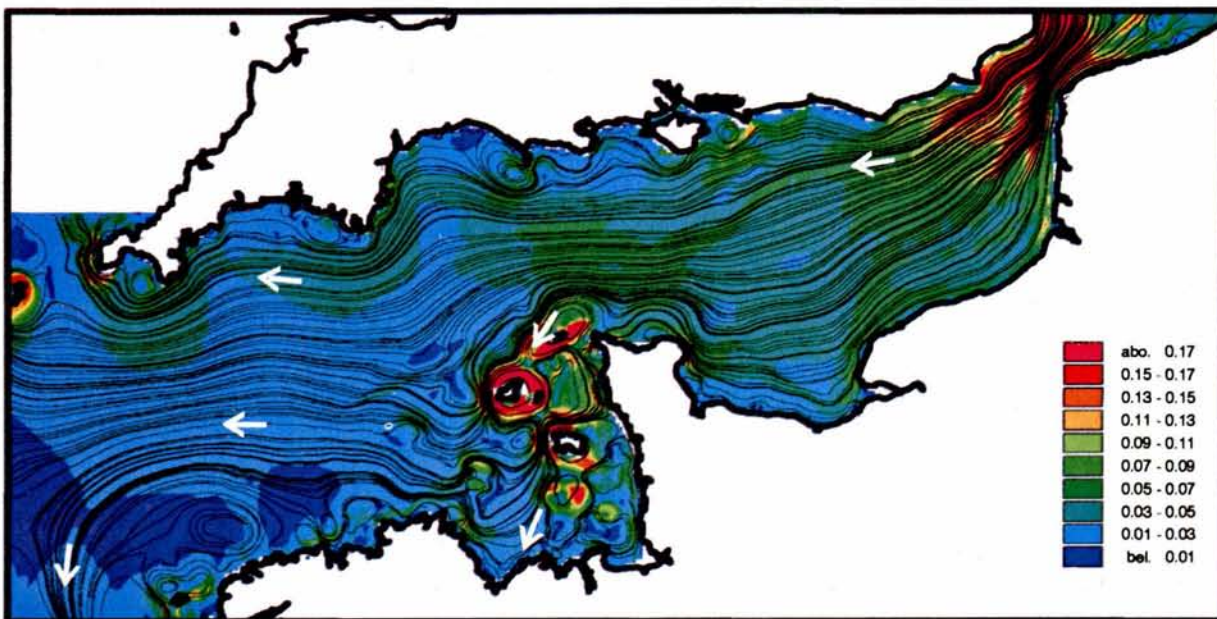


Figure 4  
Long-term trajectories and velocity of water movement for an average tide and wind stress of 0,13 Pa from the north.

Trajectoires et intensités des courants à long terme, pour une marée moyenne et une tension de vent de 0,13 Pa depuis le nord.

Figure 5

Long-term trajectories and velocity of water movement for an average tide and a wind stress of 0,13 Pa from the northeast.

Trajectoires et intensités des courants à long terme, pour une marée moyenne et une tension de vent de 0,13 Pa depuis le nord-est.

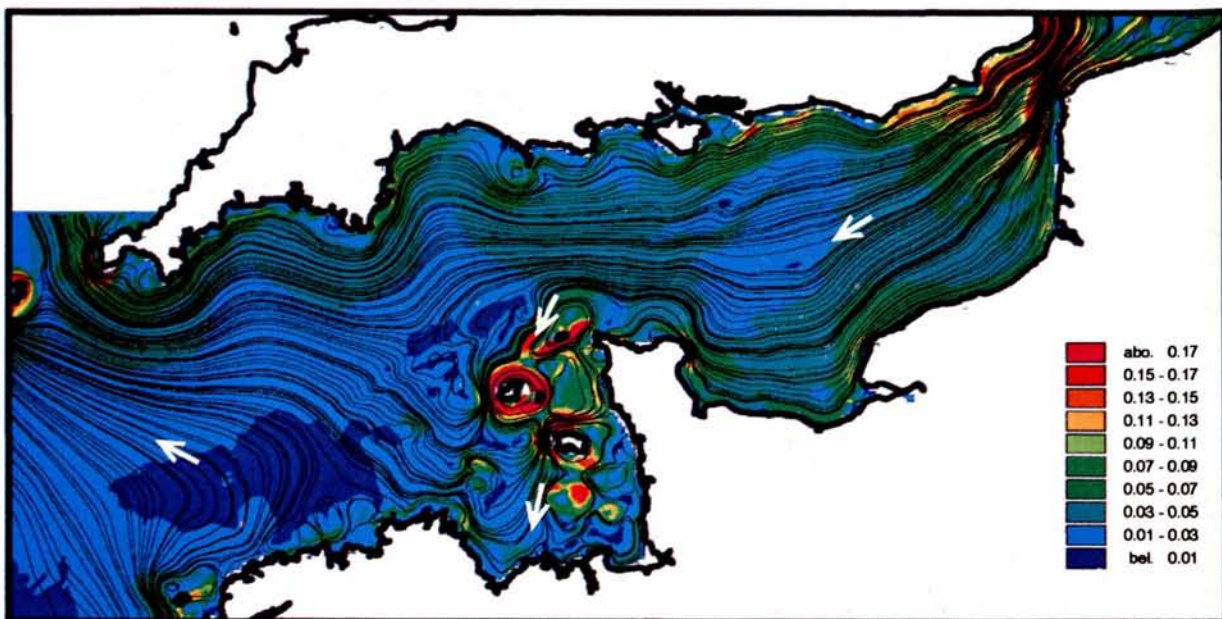


Figure 6

Long-term trajectories and velocity of water movement for an average tide and a wind stress of 0,13 Pa from the east.

Trajectoires et intensités des courants à long terme, pour une marée moyenne et une tension de vent de 0,13 Pa depuis l'est.

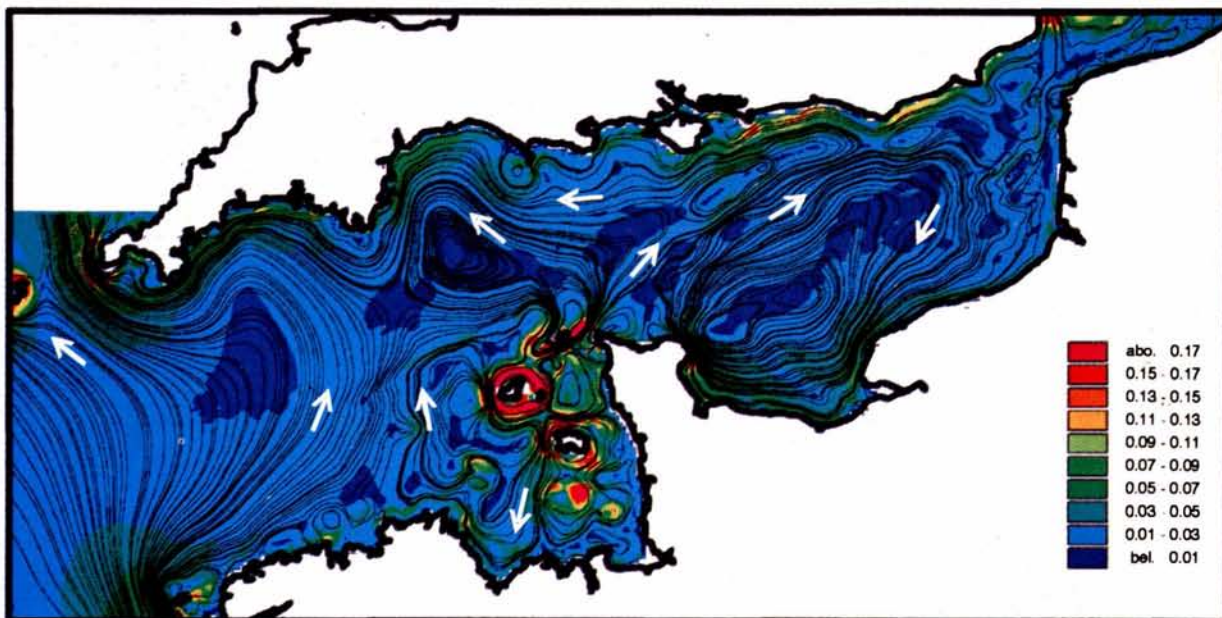
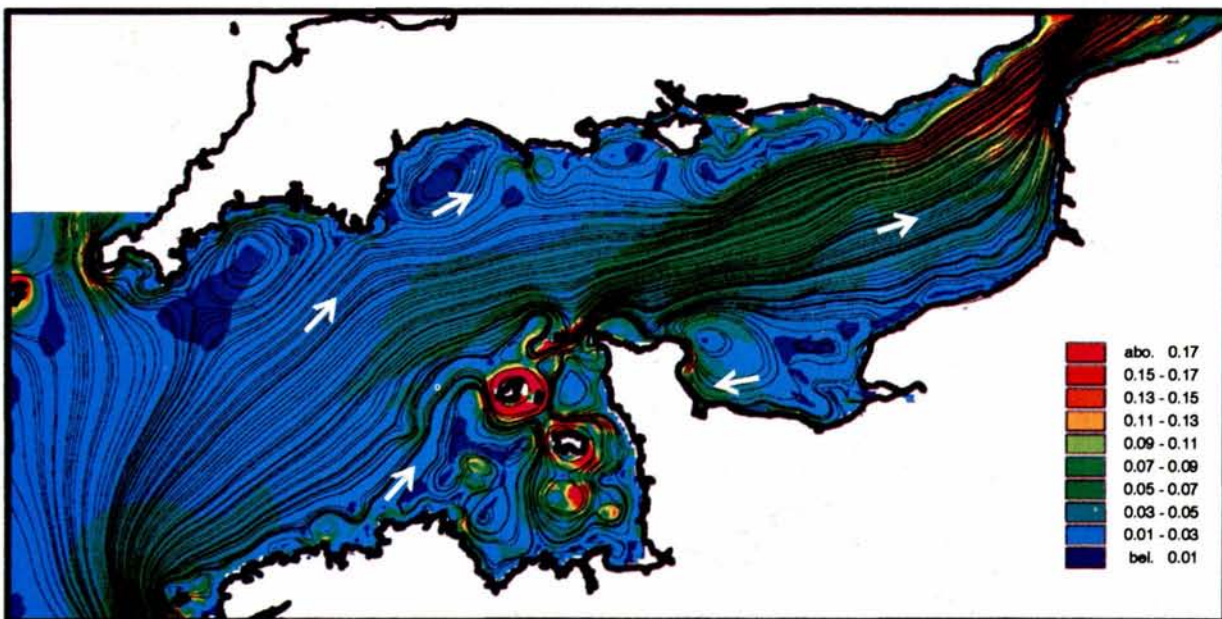


Figure 7

Long-term trajectories and velocity of water movement for an average tide and a wind stress of 0,13 Pa from the southeast.

Trajectoires et intensités des courants à long terme, pour une marée moyenne et une tension de vent de 0,13 Pa depuis le sud-est.



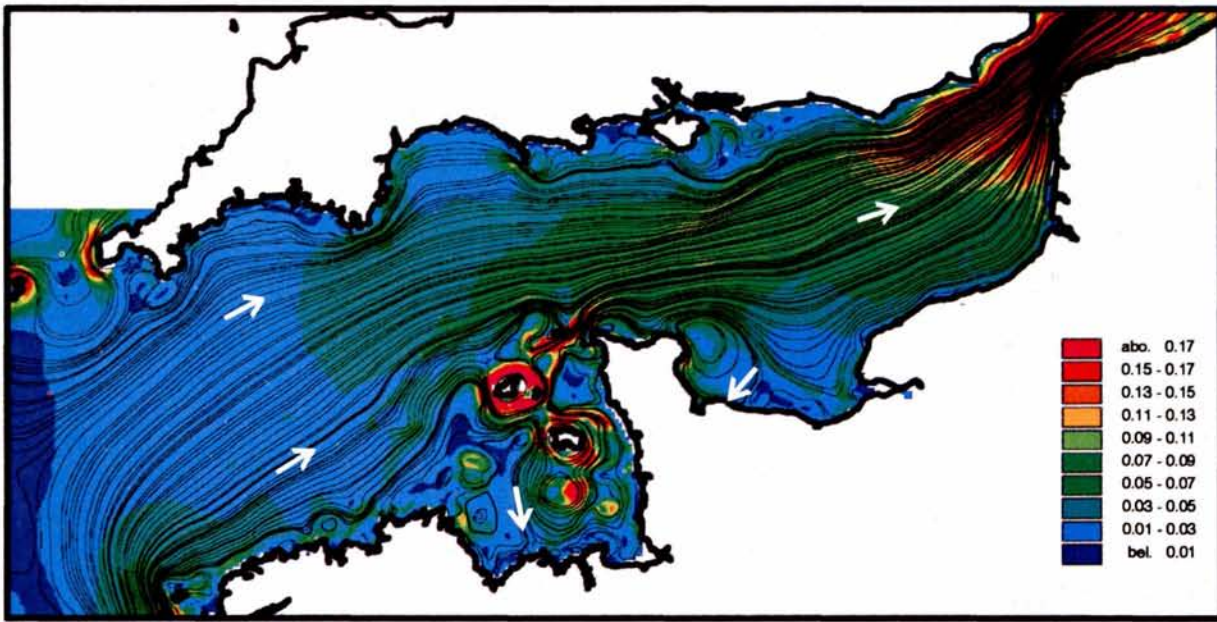


Figure 8  
 Long-term trajectories and velocity of water movement for an average tide and a wind stress of 0,13 Pa from the south.

Trajectoires et intensités des courants à long terme, pour une marée moyenne et une tension de vent de 0,13 Pa depuis le sud.

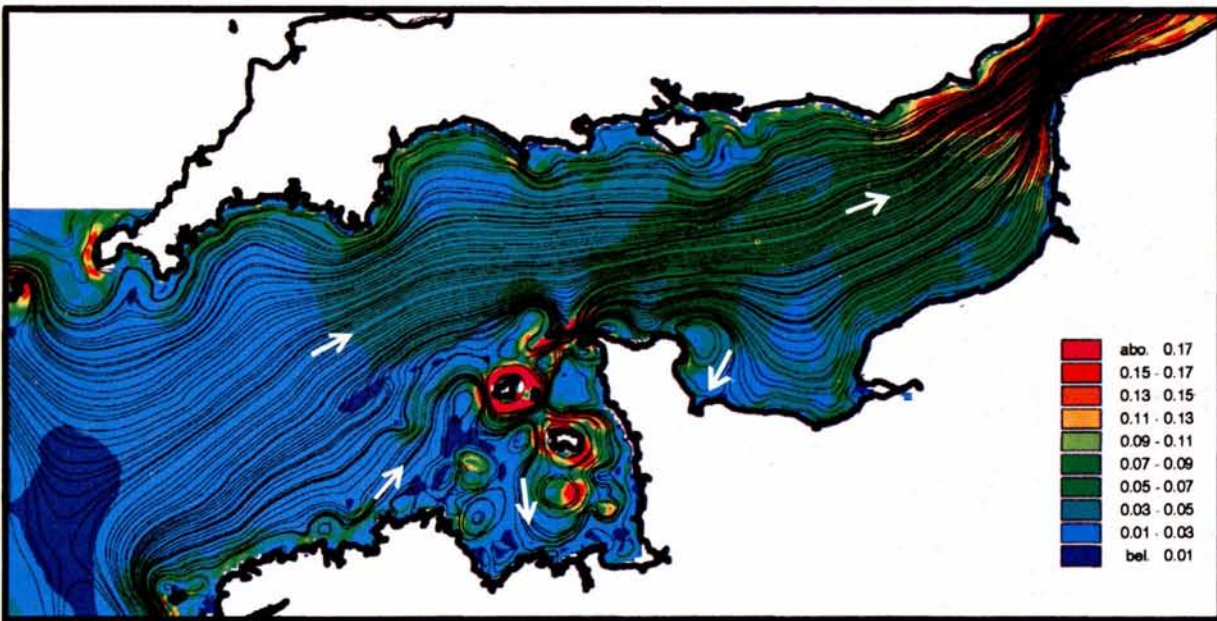


Figure 9  
 Long-term trajectories and velocity of water movement for an average tide and a wind stress of 0,13 Pa from the southwest.

Trajectoires et intensités des courants à long terme, pour une marée moyenne et une tension de vent de 0,13 Pa depuis le sud-ouest.

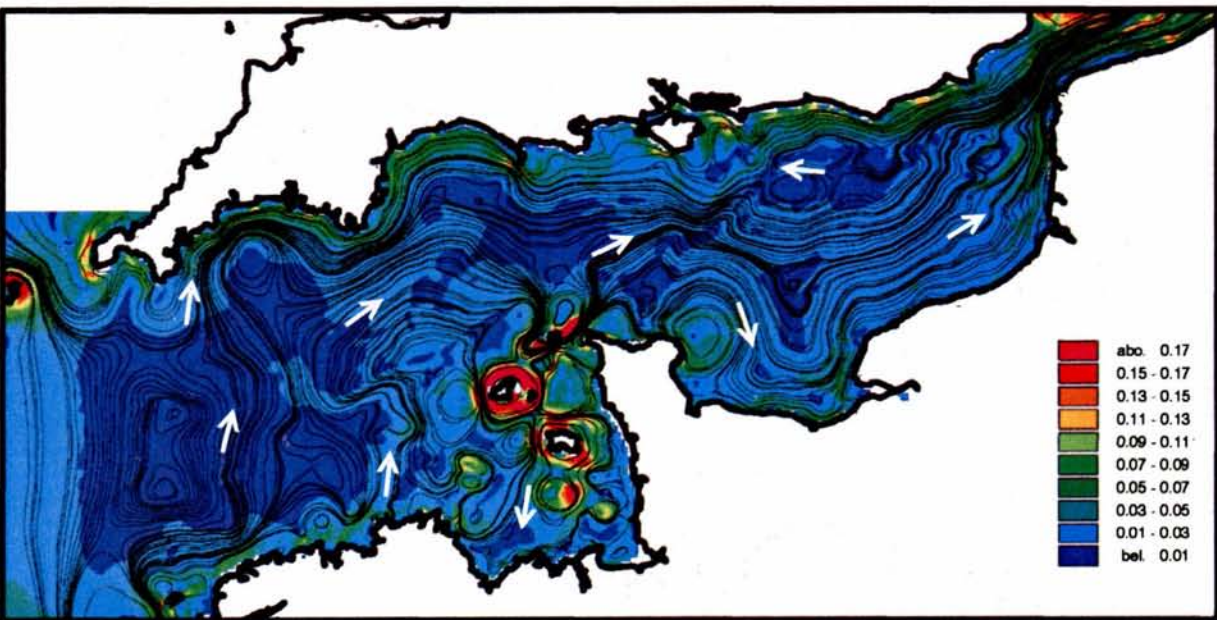


Figure 10  
 Long-term trajectories and velocity of water movement for an average tide and a wind stress of 0,13 Pa from the west.

Trajectoires et intensités des courants à long terme, pour une marée moyenne et une tension de vent de 0,13 Pa depuis l'ouest.

Figure 11

*Long-term trajectories and velocity of water movement for an average tide and a wind stress of 0,13 Pa from the northwest.*

Trajectoires et intensités des courants à long terme, pour une marée moyenne et une tension de vent de 0,13 Pa depuis le nord-ouest.

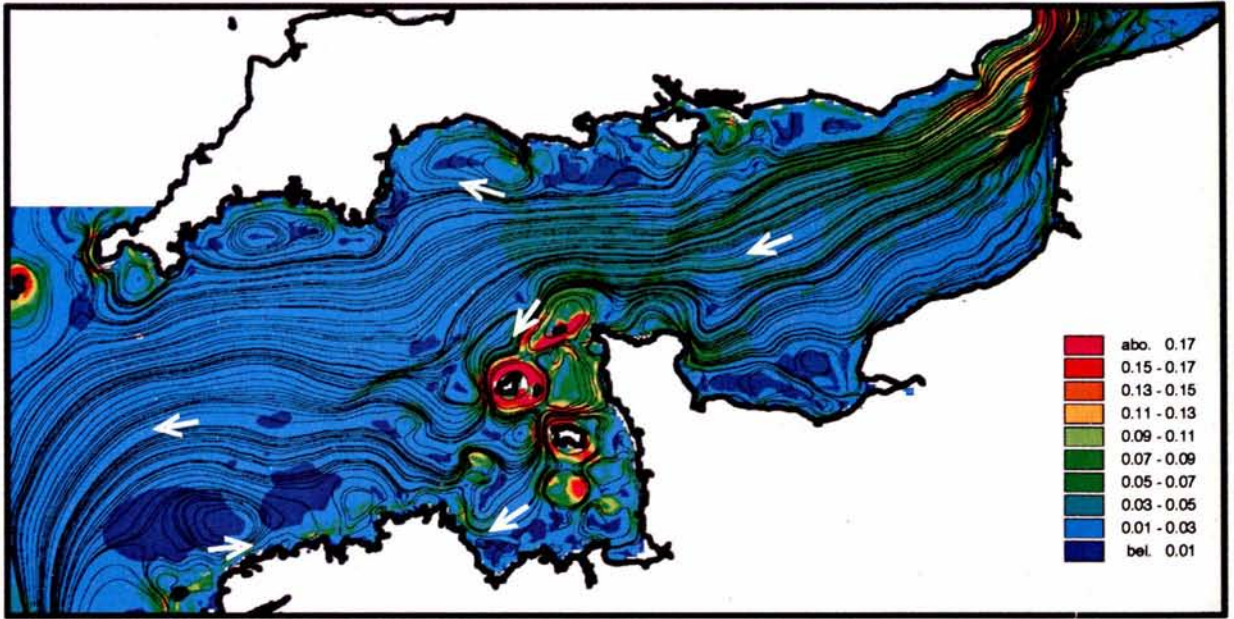


Figure 12

*Long-term trajectories and velocity of water movement in the average annual situation.*

Trajectoires et intensités des courants à long terme, en moyenne annuelle

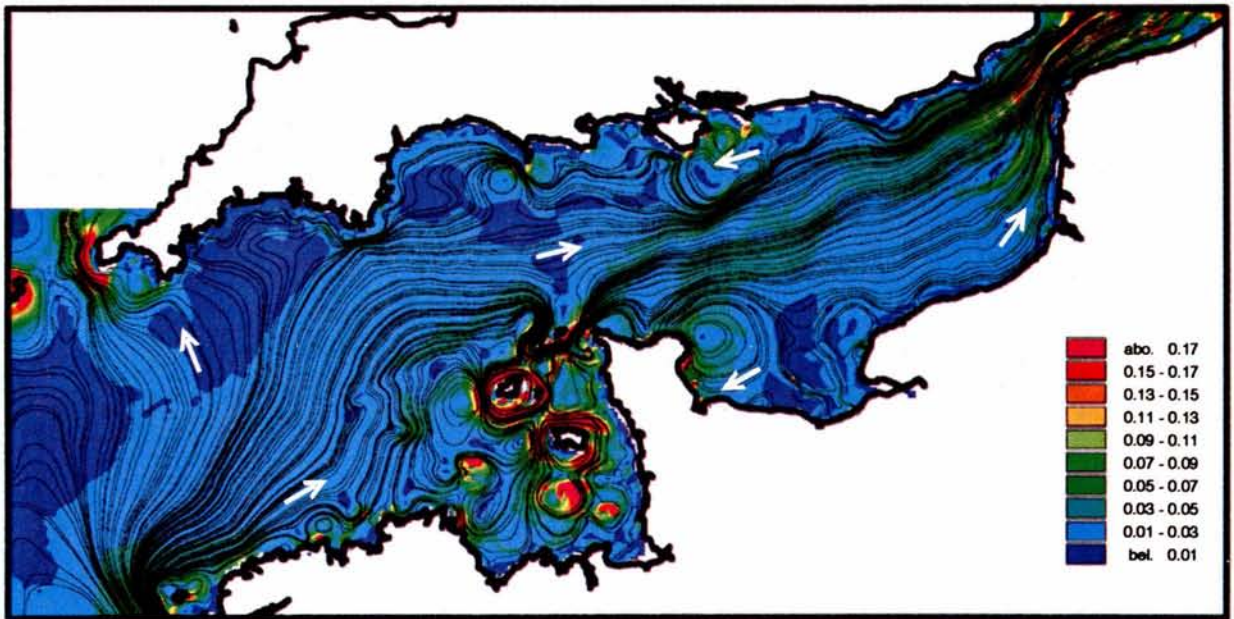
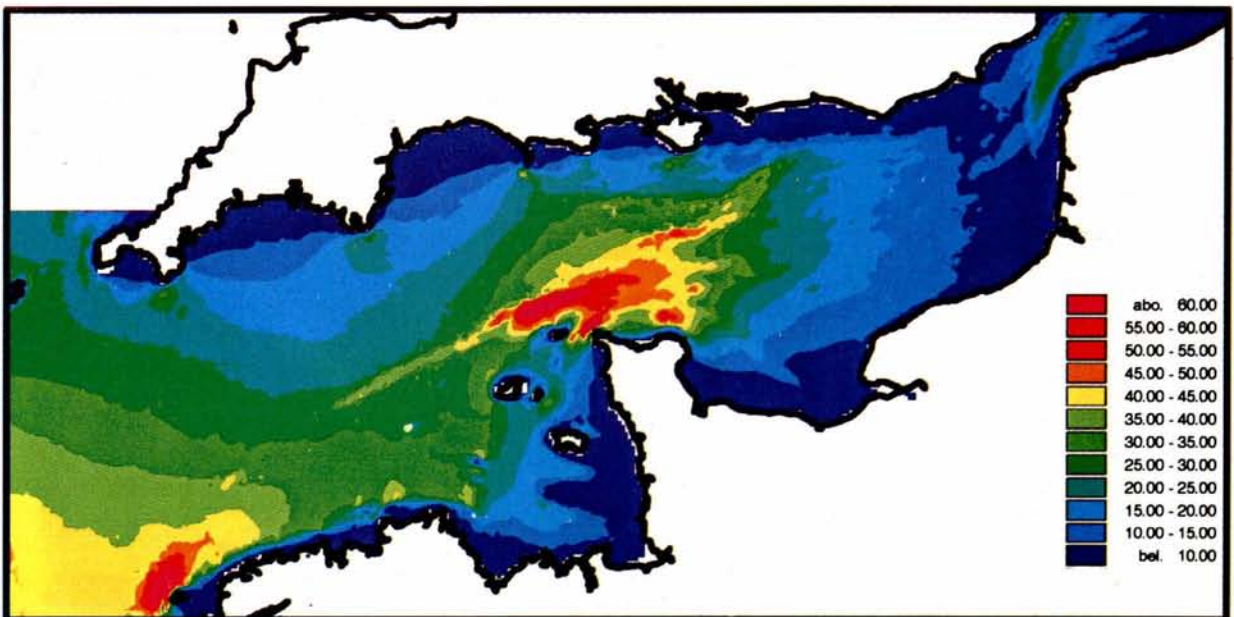


Figure 13

*Diffusion coefficient K to be used in long-term computations, in combination with Figure 12.*

Coefficient de diffusion K, à utiliser dans les calculs à long terme, en complément de la figure 12.





This is the case for the western Channel entrance in summer, for the eastern tip of the Seine Bay and the coastline of the Dover Strait.

The mean annual wind being about 5 m/s from south-southwest, the eleventh map (Fig. 12) presents this corresponding situation. This is considered to be close to the long term situation as far as currents in the Channel are concerned.

### Dispersion

Figures 2 to 12 show only the advective part of displacement of water masses and their contents. This displacement is often very slow (about one centimetre per second), so for various applications we may need to add the transport component linked to mixing (diffusion and dispersion).

This complementary step can be made using the usual mathematical laws, to be found in any study on dispersion in the hydraulic environment (for example Fisher *et al.*, 1979), using a spatially variable dispersion coefficient.

Numerical simulations of radioactive tracer dispersion in the Channel (Salomon *et al.*, 1991) showed that Elder's general law, linking the diffusion coefficient (K) to current intensity (U) and water depth (H), was applicable, subject to considering the proportionality coefficient ( $\beta$ ) as a function of the time scale, whose weather situations were representative:

$$K = \beta \overline{UH}$$

- for average weather situations over periods of about half a week,  $\beta$  would be close to 0.3;

- for average weather situations over periods of about a year,  $\beta$  would be about 0.7, which means that part of the variability of current fields is translated into an overestimation of the diffusive part.

The diagram (Fig. 13) gives the value of this coefficient K over the entire Channel, for this last case of annual averaging.

### CONCLUSION

While tidal currents are often considered to represent true currents, the diagrams shown here provide a complementary aspect of the current-related spectrum.

Tidal currents pertain to ocean movements whose characteristic scale ranges from a few seconds to a few hours. These, for instance, will interest navigation. Residual currents pertain to longer-term displacement, up to approximately two years in the Channel. These affect the movement of dissolved chemical substances and microorganisms.

Diagrams constitute a graphic means of presenting these results in such a way that a large variety of users can consult them. The same current fields also exist as digital files and can be used as a basis for mathematical models for transport and long-term dispersion.

### Acknowledgement

This work has been partly supported by EEC-MAST contracts Nos. 52 C and 53 C.

### REFERENCES

- Boxall S.R. and I.S. Robinson (1987). Shallow sea dynamics from CZCS Imagery. *Adv. Space Res.*, 7, 2, 237-246.
- Cheng R.T., S. Feng and P. Xi (1986). On Lagrangian residual ellipse. in: *Lecture notes on coastal and estuarine studies*, J. Van de Kreeke, editor. Springer-Verlag, Berlin, 102-113.
- Feng S. (1987). A three-dimensional weakly non-linear model of tide-induced Lagrangian residual current and mass-transport, with an application to the Bohai Sea. in: *Three-dimensional models of marine and estuarine dynamics*, J.C.J. Nihoul and B.P. Jamart, editors. Elsevier Oceanography Series, Amsterdam, 471-488.
- Feng S. (1990). On the Lagrangian residual velocity and the mass-transport in a multifrequency oscillatory system. in: *Coastal and Estuarine studies*, vol. 38, R.T. Cheng, editor. Residual currents and long-term transport. Springer Verlag, 34-48.
- Fisher H.B., E.J. List, R.C. Koh, J. Imberger and N.H. Brooks (1979). *Mixing in inland and coastal waters*. Academic Press, 483 pp.
- Foreman M., A. Baptista and R. Walters (1992). Tidal model studies of particle trajectories around a shallow coastal bank. *Atmos. Ocean*, 30, 1, 43-69.
- Guéguéniat P., R. Gandon, Y. Baron, J.-C. Salomon, J. Pentreath, J.-M. Brylinski and L. Cabioch (1988). Utilisation de radionucléides artificiels ( $^{125}\text{Sb}$ ,  $^{137}\text{Cs}$ ,  $^{134}\text{Cs}$ ) pour l'observation des déplacements des masses d'eau dans la Manche. in: *Radionuclides: a tool for oceanography*. Elsevier Applied Science, 260-270.
- Guéguéniat P., J.-C. Salomon, M. Wartel, L. Cabioch and A. Fraizier (1993 b). Transfer pathways and transit time of dissolved matter in the eastern English Channel indicated by space-time radiotracer measurement and hydrodynamic modelling. *Estuar. coast. Shelf Sci.*, 36, 477-494.
- Jégou A.-M. and J.-C. Salomon (1991). Hydrodynamique côtière: couplage images satellitaires-modèles numériques. Application à la Manche. *Proceedings of the International Colloquium on the environment of epicontinental seas*, Lille, 20-22 March 1990, *Oceanologica Acta*, Vol. sp. n° 11, 55-61.
- Longuet-Higgins M.S. (1969). On the transport of mass by time-varying ocean currents. *Deep-Sea Res.*, 16, 431-447.
- Miche M. (1944). Mouvements ondulatoires de la mer en profondeur constante ou décroissante. *Annls Ponts et Chaussées*, 2, 25-61.
- Orbi A. and J.-C. Salomon (1988). Dynamique de marée dans le golfe normand-breton. *Oceanologica Acta*, 11, 1, 55-64.

- Pingree R.D.** (1984). Some applications of remote sensing to studies in the Bay of Biscay, Celtic Sea and English Channel. in: *Remote Sensing of Shelf Sea Hydrodynamics*, J.C.J. Nihoul, editor. Elsevier Oceanography series, 38, 287-315.
- Pingree R.D et L. Maddock** (1977). Tidal residual in the English Channel. *J. mar. biol. Ass. U.K.*, **57**, 339-354.
- Pingree R.D et L. Maddock** (1985). Stokes, Euler and Lagrange aspects of residual tidal transports in the English Channel and the southern bight of the North Sea. *J. mar. biol. Ass. U.K.*, **65**, 969-982.
- Pingree R.D et G.T. Mardell** (1987). Tidal flows around the Channel Islands. *J. mar. biol. Ass. U.K.*, **67**, 691-707.
- Ridderinkhof H. and J.T.F. Zimmerman** (1992). Chaotic stirring in a tidal system. *Science*, **258**, 1107-1111.
- Ronday F.** (1976). Modèles hydrodynamiques, modélisation des systèmes marins, projet mer, rapport final. Services du Premier Ministre, Bruxelles, Belgique, Vol. 3, 270 pp.
- Salomon J.-C. and M. Breton** (1991). Courants résiduels de marée dans la Manche. *Proceedings of the International Colloquium on the environment of epicontinental seas, Lille, 20-22 March 1990*, *Oceanologica Acta*, Vol. sp. No. 11, 47-53.
- Salomon J.-C., P. Guéguéniat, A. Orbi and Y. Baron** (1988). A Lagrangian model for long-term tidally-induced transport and mixing. Verification by artificial radionuclide concentrations. in: *Radionuclides: a tool for oceanography*. Elsevier Applied Science, 384-394.
- Salomon J.-C., P. Guéguéniat and M. Breton** (1991). Mathematical model of  $^{125}\text{Sb}$  transport and dispersion in the Channel. in: *Radionuclides in the study of marine processes*, P.J. Kershaw and D.S. Woodhead, editors. Elsevier Applied Science, 74-83.
- Salomon J.-C., M. Breton and P. Guéguéniat** (1993 a). Computed residual flow through the Strait of Dover. *Channel Symposium, 1992, Oceanologica Acta*, **16**, 5-6, 449-455 (this issue).
- Salomon J.-C., P. Garreau and M. Breton** (1993 b). The Lagrangian barycentric method to compute 2D and 3D long-term dispersion in tidal environments. in: *Mixing processes in estuaries and coastal seas*, C. Pattiaratchi, editor. AGU Series (in press).
- Service Hydrographique et Océanographique de la Marine** (1973). Courants de marée de Dunkerque à Brest. Service Hydrographique et Océanographique de la Marine, 20 pp.
- Schwiderski E.W.** (1983). Atlas of ocean tidal charts and maps. *Mar. Geod.*, **6**, 219-265.
- Zimmerman J.T.F.** (1979). On the Euler-Lagrange transformation and the Stokes's drift in the presence of oscillatory and residual currents. *Deep-Sea Res.*, **26 A**, 505-520.